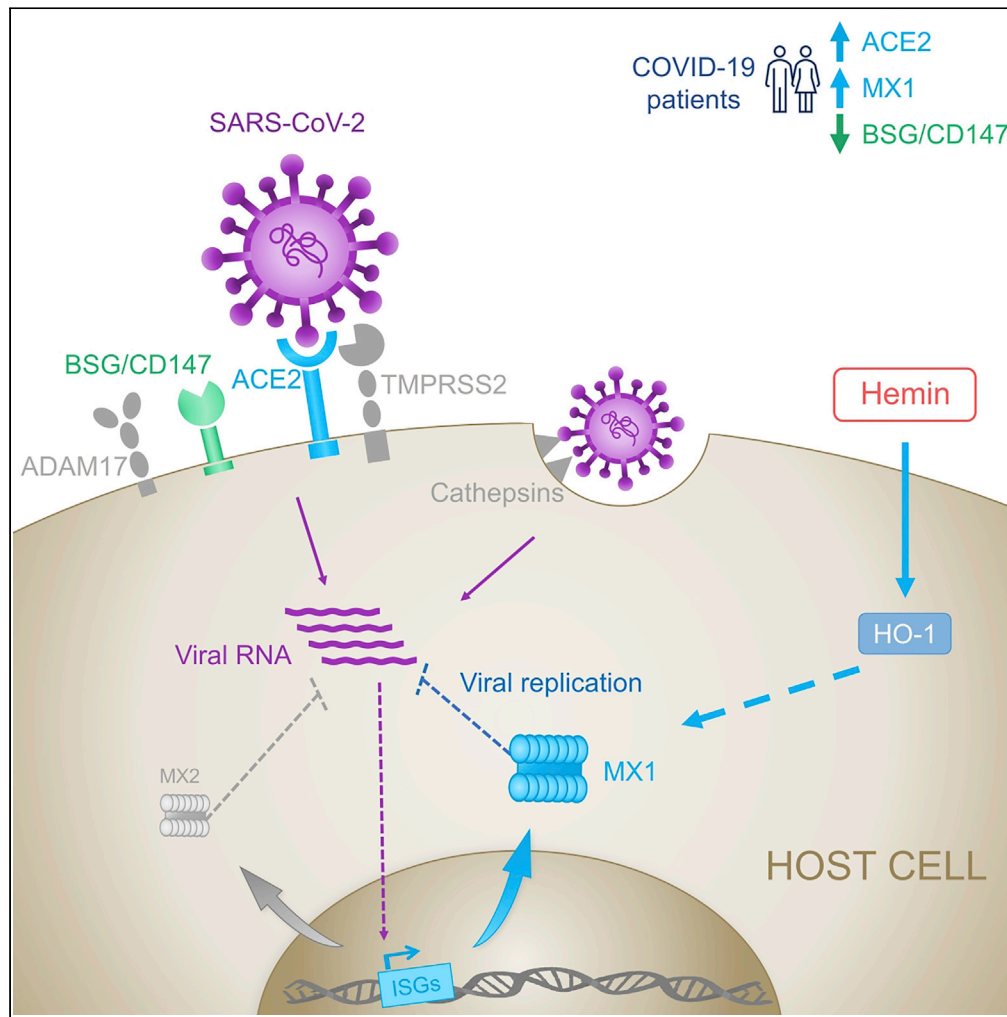**Article**

SARS-CoV-2 Infection Boosts *MX1* Antiviral Effector in COVID-19 Patients

Juan Bizzotto,
Pablo Sanchis,
Mercedes
Abbate, ..., Elba
Vazquez, Javier
Cotignola,
Geraldine Gueron

elba@qb.fcen.uba.ar (E.V.)
jcotignola@qb.fcen.uba.ar
(J.C.)
ggueron@iquibicen.fcen.uba.
ar (G.G.)

HIGHLIGHTS

COVID-19 patients
present a distinct
expression pattern for
antiviral genes

MX1 antiviral gene
expression is triggered by
SARS-CoV-2

MX1 can be induced by
hemin, an FDA-approved
drug

MX1 rises as a potential
druggable target

iScience

Article

SARS-CoV-2 Infection Boosts *MX1* Antiviral Effector in COVID-19 Patients

Juan Bizzotto,[1,2,3] Pablo Sanchis,[1,2,3] Mercedes Abbate,[1,2,3] Sofía Lage-Vickers,[1,2,3] Rosario Lavignolle,[1,2,3] Ayelén Toro,[1,2,3] Santiago Olszevicki,[1,2] Agustina Sabater,[1,2] Florencia Cascardo,[1,2] Elba Vazquez,[1,2,*] Javier Cotignola,[1,2,*] and Geraldine Gueron[1,2,4,*]

SUMMARY

In a published case-control study (GSE152075) from SARS-CoV-2-positive (n = 403) and -negative patients (n = 50), we analyzed the response to infection assessing gene expression of host cell receptors and antiviral proteins. The expression analysis associated with reported risk factors for COVID-19 was also assessed. SARS-CoV-2 cases had higher *ACE2*, but lower *TMPRSS2*, *BSG/CD147*, and *CTSB* expression compared with negative cases. COVID-19 patients' age negatively affected *ACE2* expression. *MX1* and *MX2* were higher in COVID-19 patients. A negative trend for *MX1* and *MX2* was observed as patients' age increased. Principal-component analysis determined that *ACE2*, *MX1*, *MX2*, and *BSG/CD147* expression was able to cluster non-COVID-19 and COVID-19 individuals. Multivariable regression showed that *MX1* expression significantly increased for each unit of viral load increment. Altogether, these findings support differences in *ACE2*, *MX1*, *MX2*, and *BSG/CD147* expression between COVID-19 and non-COVID-19 patients and point out to *MX1* as a critical responder in SARS-CoV-2 infection.

INTRODUCTION

Severe acute respiratory syndrome coronavirus 2 (SARS-CoV-2) is a novel virus that emerged in late 2019 in Wuhan, China (World Health Organization, 2020). The World Health Organization (WHO) declared the SARS-CoV-2 infection a pandemic health emergency as of January 31, 2020.

As of July 28, 2020, there are 16,812,755 confirmed cases of COVID-19 (coronavirus disease 2019), including 662,905 deaths reported to WHO from 216 countries and territories. The current worldwide COVID-19 fatality rate (4%) is lower than that of SARS-CoV-1 (10%) and Middle East respiratory syndrome (MERS)-CoV (32%) (World Health Organization, 2020). However, the total number of infected and dead people is much higher than that due to the latter viruses.

Analyses for viral stability in aerosols and surfaces showed high similarity among SARS-CoV-2 and SARS-CoV-1 (van Doremalen et al., 2020). This might imply that the differences in the epidemiologic viral features probably arise from viral and host factors such as sex, comorbidities (Zheng et al., 2020), higher viral loads, and/or the potential for asymptomatic individuals to spread the virus (Bai et al., 2020; Zou et al., 2020).

SARS-CoV-2 invades host cells mainly via two receptors: angiotensin-converting enzyme 2 (ACE2) (Letko et al., 2020; Yan et al., 2020) and Basigin or EMMPRIN (BSG/CD147) (Wang et al., 2020). This mechanism results from the interaction between the host receptors and the viral spike glycoproteins (S), after priming of this viral protein by the serine protease TMPRSS2 (Hoffmann et al., 2020). TMPRSS2 inhibition has been shown to block SARS-CoV-2 cell entry (Hoffmann et al., 2020). In addition to ACE2, Wang et al. (2020) demonstrated that SARS-CoV-2 S protein also binds to BSG/CD147 (Ulrich and Pillat, 2020).

Sequential protease cleavage models have been proposed for activation of S protein of SARS-CoV and MERS-CoV (Belouzard et al., 2009; Millet and Whittaker, 2014). Depending on the virus strain and the

[1]Universidad de Buenos Aires, Facultad de Ciencias Exactas y Naturales, Departamento de Química Biológica, Intendente Guiraldes 2160, Buenos Aires, C1428EGA, Argentina

[2]CONICET - Universidad de Buenos Aires, Instituto de Química Biológica de la Facultad de Ciencias Exactas y Naturales (IQUIBICEN), Buenos Aires, C1428EGA, Argentina

[3]These author contributed equally

[4]Lead Contact

*Correspondence:
elba@qb.fcen.uba.ar (E.V.),
jcotignola@qb.fcen.uba.ar (J.C.),
gueron@iquibicen.fcen.uba.ar (G.G.)

https://doi.org/10.1016/j.isci.2020.101585

cell types infected, S protein may be cleaved by one or several host proteases, including cathepsins, TMPRSS2, and BSG/CD147 (Park et al., 2016; Ulrich and Pillat, 2020). Thus, coronavirus cell entry, either through plasma membrane or endocytosis, appears to be largely determined by the availability of these proteases (Ou et al., 2020).

Of note, ADAM metallopeptidase domain 17 (ADAM17) may exert a protective effect on SARS-CoV-2 infection. ADAM17 can release the ectodomains of a plethora of membrane-anchored factors, such as ACE2 (Lambert et al., 2005; Palau et al., 2020).

However, the lead roles of these factors in promoting viral infection in humans still remain elusive.

Although much attention has been placed in virus host cell receptors, little has been commented on antiviral effector proteins. It is well accepted that type I interferon (IFN) is essential in fighting viral infection by induction of IFN-stimulated genes (ISGs), which work in synergy to inhibit viral replication via multiple mechanisms (Li et al., 2018; Teijaro, 2016). The human myxovirus resistance genes (*MX*) encode GTPases that are part of the antiviral response induced by type I/III IFNs (Verhelst et al., 2012). Humans encode two different MX proteins, MX1 and MX2, which differ considerably in viral specificities and mechanisms of action. MX1 has been shown to have wide antiviral activity against RNA and DNA viruses (Haller et al., 2015), whereas MX2 action is limited to certain viruses such as HIV (Bhargava et al., 2018). Specifically, MX1 has a direct effect on the viral ribonucleoprotein complex and its GTPase activity is essential for its antiviral function. Greater MX1 expression correlated with better response to influenza A H1N1 pandemic in 2009 (Verhelst et al., 2012).

The main therapeutic avenues to halt respiratory virus infection are targeting the virus directly or targeting the host system. Although the first strategy is highly efficient, it is limited by the sensitivity/resistance of the virus strain (McKimm-Breschkin, 2005; Monto, 2003). On the other hand, the second strategy is impaired by having shown relatively low efficacy (Darwish et al., 2011; Ramos and Fernandez-Sesma, 2015). As the clinical picture has evidenced that the "cytokine storm" triggered by these viruses causes severe lung injury and lethality (Jose and Manuel, 2020), and that antiviral drugs are not effective in preventing such lung injury, it is imperative to spawn new drugs that have the capacity to boost the host immune response while controlling tissue damage as a consequence of these infections (Zheng et al., 2008).

There are no conclusive data evidencing the shifts in expression of host cell receptors and viral effectors produced by SARS-CoV-2 infection in humans. Thus, in this work we analyzed gene expression profiles in response to coronavirus infection in COVID-19 versus non-COVID-19 patients. We evaluated the expression of the main host cell receptors described for SARS-CoV-2 and potential antiviral genes. Our results evidence high discrepancies regarding the expression of the reported main viral host cell receptors associated with COVID-19, and point out to the relevance of MX1 to fight this disease.

RESULTS

Expression of Host Cell Receptors in SARS-CoV-2-Positive and -Negative Patients

We used the publicly available RNA sequencing (RNA-seq) dataset GSE152075 to evaluate the expression of known host SARS-CoV-2 receptor genes: *ACE2*, *TMPRSS2*, *BSG/CD147*, *CTSB*, *CTSL*, and *ADAM17* (Heurich et al., 2014; Hoffmann et al., 2020; Simmons et al., 2005; Ulrich and Pillat, 2020; Zhou et al., 2015). This set consists of transcriptome data from nasopharyngeal swabs from 430 SARS-CoV-2-positive and 54 SARS-CoV-2-negative patients. We excluded 27 SARS-CoV-2-positive and 4 SARS-CoV-2-negative samples from the downstream analyses because the RNA-seq data from these individuals was of low quality (>70% of genes resulting in 0 sequencing reads). Patient demographics are available in Table S1.

Results evidenced that COVID-19 patients had higher *ACE2* expression compared with non-COVID-19 patients (Figure 1A.I; p = 1.7×10^{-7}). On the contrary, *TMPRSS2* (Figure 1B.I), *BSG/CD147* (Figure 1C.I), and *CTSB* (Figure 1D.I) expression was lower in the COVID-19 group (p = 3.4×10^{-9}, p = 2.0×10^{-12}, and p = 6.8×10^{-9}, respectively). Non-statistical differences for *CTSL* and *ADAM17* expression were observed between SARS-CoV-2-positive and -negative patients (Figures 1E.I and 1F.I, respectively).

As the reported risk factors for SARS-CoV-2 infection include age and sex, we next assessed the association between these risk factors and the host receptors' gene expression. We did not find gene expression
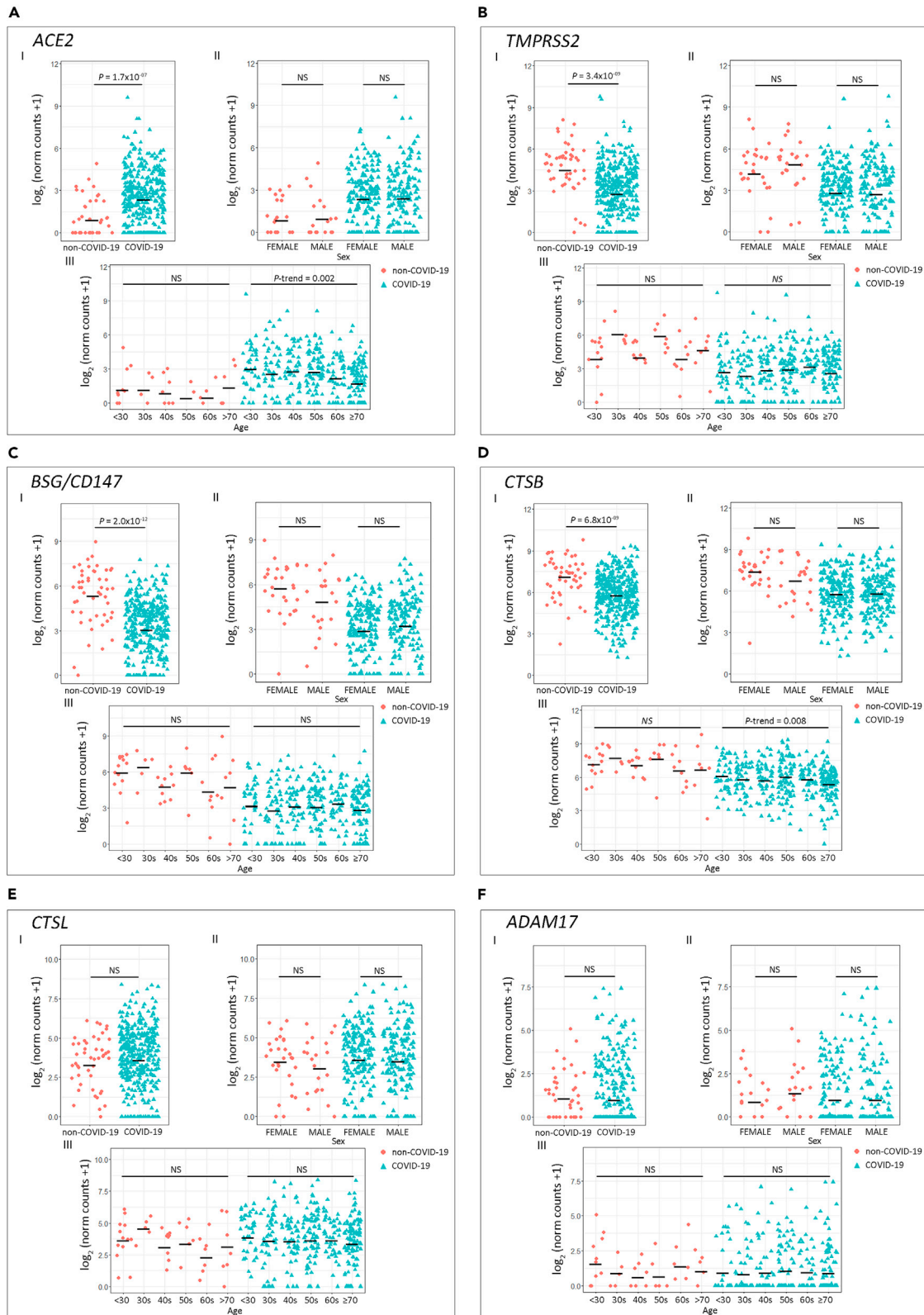
Figure 1. Expression of Host Cell Receptor Genes in COVID-19 and Non-COVID-19 Patients

(A–F) Gene expression analysis for host cell receptor genes (A) *ACE2*, (B) *TMPRSS2*, (C) *BSG/CD147*, (D) *CTSB*, (E) *CTSL*, and (F) *ADAM17*.

(I) COVID-19 versus non-COVID-19 patients (p values correspond to Wilcoxon rank-sum test); (II) COVID-19 and non-COVID-19 patients by sex (p values correspond to Wilcoxon rank-sum test); (III) COVID-19 and non-COVID-19 patients categorized by age groups (p values correspond to decreasing Jonckheere-Terpstra trend test). Statistical significance was set at p < 0.05. NS: not significant.

differences between sex (Figures 1A.II–1F.II). When analyzing the association between gene expression and age, we found that the older the COVID-19 patient, the lower the expression for *ACE2* (Figure 1A.III; P-trend$_{decreasing}$ = 0.002) and *CTSB* (Figure 1D.III; P-trend$_{decreasing}$ = 0.008). We did not observe an association between age and gene expression for the other receptors in the COVID-19 group (Figures 1B.III, 1C.III, 1E.III, and 1F.III). For SARS-CoV-2-negative donors, no variation in gene expression associated with age was observed (Figures 1A.III–1F.III).

**Expression of Antiviral-Associated Genes in SARS-CoV-2-Positive and -Negative Patients**

Next, we assessed antiviral-associated genes that play a crucial role in halting viral replication via multiple mechanisms: *MX1*, *MX2*, *NRF2*, *IRF3*, *HIF1A*, and *HMOX1* (Chiang and Liu, 2018; Espinoza et al., 2017; Haller et al., 2015; Hassan et al., 2020; Hong et al., 2009) (Figure 2). *MX1* (Figure 2A.I) and *MX2* (Figure 2B.I) expression was significantly higher in COVID-19 patients (p = 7.2×10^{-11} and p = 2.3×10^{-13}, respectively) compared with the non-COVID-19 group. No significant differences were observed between patients of different sex for any of the genes assessed (Figures 2A.II–2F.II). Interestingly, we observed a negative trend for *MX1* (Figure 2A.III; P-trend$_{decreasing}$ = 0.004) and *MX2* (Figure 2B.III; P-trend$_{decreasing}$ = 0.012) expression as patients' age increased. In addition, *NRF2* and *IRF3* expression was significantly lower in COVID-19 patients (Figures 2C.I and 2D.I; p = 0.010 and p = 5.0×10^{-4}, respectively), and *NRF2* also showed a significant P-trend in COVID-19 patients grouped by age (Figure 2C.III; P-trend$_{decreasing}$ = 0.004). No statistical differences were observed when comparing *HMOX1* and *HIF1A* expressions (Figures 2E and 2F). For SARS-CoV-2-negative donors no variation in gene expression associated with age was observed (Figures 2A.III–2F.III).

Gene Correlation and Principal-Component Analysis

Next, we performed pairwise Spearman correlation analyses (Figure 3A and Table S2) for host receptors and antiviral gene expression levels of the host receptors and antiviral genes. We considered all patients (Corr.), only non-COVID-19 patients (Neg.), and only COVID-19 patients (Pos.). Black boxes highlight statistically significant correlation among genes for COVID-19 patients, whereas correlations for the same pairs in non-COVID-19 patients appeared non-significant (Figure 3A). Of note, *ACE2* showed an r = 0.416 (p < 1×10^{-15}) with *MX1*, whereas *MX2* showed an r = 0.423 (p < 1×10^{-15}) with *HMOX1*, an r = 0.595 (p < 1×10^{-15}) with *CTSB*, and an r = 0.450 (p < 1×10^{-15}) with *CTSL* (Figure 3A and Table S2).

Interestingly, although *MX1* and *MX2* respond to SARS-CoV-2 infection (Figures 2A and 2B), the correlation analysis highlights *MX2* positive correlation for both non-COVID-19 and COVID-19 patients (Figure 3A and Table S2; r = 0.642, p = 4.97×10^{-7} and r = 0.899, p < 1×10^{-15}, respectively), whereas *MX1* only displays positive correlation for COVID-19 patients. These data suggest that *MX1* might be more specific in the response to SARS-CoV-2 than *MX2*.

In parallel, we performed a principal-component analysis (PCA), which is a dimensionality reduction technique, used to increase the interpretability of the dataset, minimizing at the same time information loss and maximizing variance. In this dataset, the principal component (PC) 1 explained 43.8% of the variance among samples (Figure 3B). Only the infection status is shown because none of the other assessed variables (age, sex, and RNA-seq batch) clustered the samples on PC1. The PC2 is responsible for 13.1% of the variability, and the expression of *ACE2*, *MX1*, *MX2*, and *BSG/CD147* seemed to drive the difference between non-COVID-19 and COVID-19 individuals (Figure 3B). Furthermore, we plotted the combined expression of *ACE2*, *BSG/CD147*, and *MX1* (Figure 3C.I) and *ACE2*, *BSG/CD147*, and *MX2* (Figure 3C.II). These combinations were selected because *MX1* and *MX2* gene expression were highly correlated for both non-COVID-19 and COVID-19 patients (Figure 3A and Table S2). The graphs show distinct 95% confidence ellipsoids, generated by 3-gene expression patterns, able to cluster non-COVID-19 and COVID-19 individuals (Figure 3C).
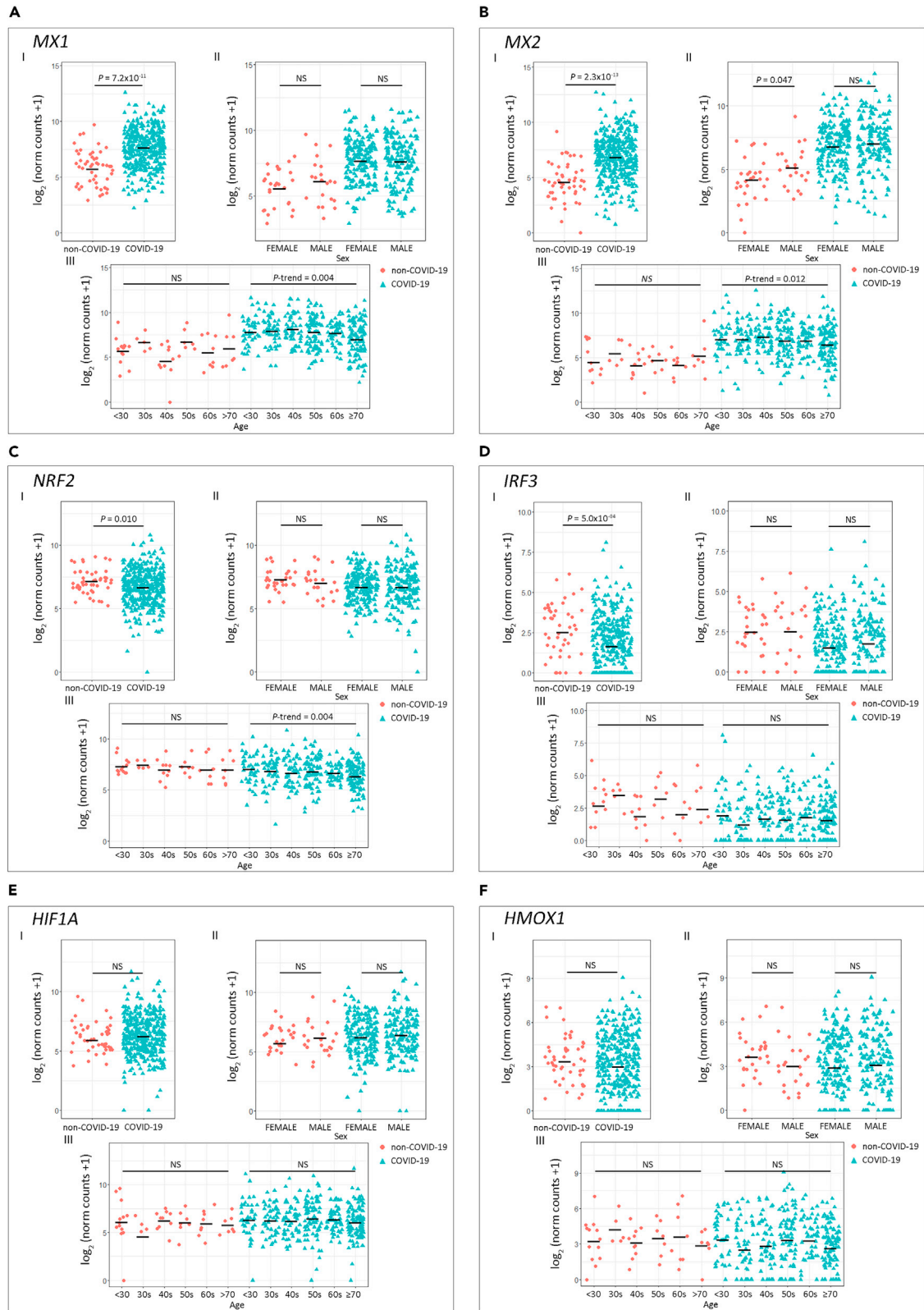
Figure 2. Expression of Host Antiviral Effector Genes in COVID-19 and Non-COVID-19 Patients

(A–F) Gene expression analysis for the selected host cell receptor genes (A) *MX1*, (B) *MX2*, (C) *NRF2*, (D) *IRF3*, (E) *HIF1A,* and (F) *HMOX1*.

(I) COVID-19 versus non-COVID-19 patients (p values correspond to Wilcoxon rank-sum test), (II) COVID-19 and non-COVID-19 patients by sex (p values correspond to Wilcoxon rank-sum test), and (III) COVID-19 and non-COVID-19 patients categorized by age groups (p values correspond to decreasing Jonckheere-Terpstra trend test). Statistical significance was set at p < 0.05. NS: not significant.

SARS-CoV-2 Viral Load Association with Gene Expression

To assess the correlation between gene expression and SARS-CoV-2 viral load, we used the PCR cycle threshold (Ct) of the N1 viral gene amplification as a surrogate variable for viral load. We found a positive correlation between expression of *ACE2* (Figure 4A.I; r = 0.260, p = 2.6×10^{-7}), *CTSL* (Figure 4A.I; r = 0.110, p = 0.034), *MX1* (Figure 4A.II; r = 0.230, p = 7.1×10^{-6}), and *MX2* (Figure 4A.II; r = 0.190, p = 2.0×10^{-4}), with SARS-CoV-2 viral load. Of note, *MX1* correlation with viral load appears to be stronger than the correlation observed for *MX2*, further supporting *MX1* enhanced response to SARS-CoV-2, compared with *MX2*. On the other hand, we observed a negative correlation between *BSG/CD147* expression (Figure 4A.I; r = −0.120, p = 0.015) and viral load. These results were further supported by PCA that showed a rough clustering of COVID-19 samples according to patients' viral load (high, medium, low) mainly by *ACE2*, *BSG/CD147*, *MX1*, and *MX2* (Figure 4B).

Next, we analyzed the pairwise correlations for *BSG/CD147, ACE2, MX1,* and *MX2* considering viral load in COVID-19 patients. As expected, results showed positive and significant correlations for all genes in all comparisons (Figure 5A). Although a high correlation was observed for *MX1* versus *MX2* + viral load (Figure 5A; r = 0.907, p = 2.2×10^{-16}), this is probably due to the collinearity between *MX1* and *MX2*.

Finally, we assessed the association between each gene with viral load using a linear multivariable regression analysis adjusted by age. Results indicate that viral load can explain variations in *MX1, BSG/CD147,* and *ACE2* expression (Figure 5B.I; p = 0.004, p = 0.038, and p = 0.084, respectively). However, *MX2* does not appear to behave dependently from viral load when considering patient's age (Figure 5B.I; p = 0.590). When further adjusting the model to consider the viral load-dependent genes, we found that for each unit of increase in viral load, *MX1* expression increased 26.76 units, *ACE2* expression increased 1.03 units, and *BSG/CD147* expression decreased 1.35 units (Figure 5B.II; p < 0.001, p = 0.170 and p < 0.001, respectively). Altogether these results point out to *MX1* as the critical responder in SARS-CoV-2 infection.

## DISCUSSION

Respiratory epithelium is the primary barrier that defends the host against respiratory pathogens. When respiratory viruses overcome the first barrier, attachment and internalization into epithelial cells is the next step to start its replication.

ACE2 mediates SARS-CoV-2 entry to the cells by binding to the S protein (Hoffmann et al., 2020). Its primary physiological function is the conversion of angiotensin II to angiotensin-(1–7). There are controversial data concerning therapies that could modulate ACE2 expression, like angiotensin receptor blockers (ARBs), as they may cause an initial up-regulation with further down-regulation of ACE2 expression during SARS-CoV-2 infection, still not ascertaining whether this may lead to harmful or beneficial effects (Vaduganathan et al., 2020). Our analysis evidenced an increase of *ACE2* expression in COVID-19 versus non-COVID-19 patients correlating with viral load.

TMPRSS2 is currently also in the main scene regarding key SARS-CoV-2 host cell receptors (Hoffmann et al., 2020). TMPRSS2-mediated cleavage of S protein has been described to be necessary for SARS-CoV and MERS-CoV productive infections (Glowacka et al., 2011; Matsuyama et al., 2010; Shulla et al., 2011). Recently, this same process has been reported for SARS-CoV-2 (Hoffmann et al., 2020). However, our analysis reflects a down-regulation of *TMPRSS2* in COVID-19 patients. Similarly, *BSG/CD147*, another receptor that binds to the S protein (Wang et al., 2020), appears to be down-regulated in COVID-19 patients with lower levels associated with higher viral load. These results may suggest that SARS-CoV-2 infection may prompt a selective mechanism of host cell receptors, and thus, targeting TMPRSS2 and BSG/CD147 might not necessarily be the most effective strategy to halt infection.
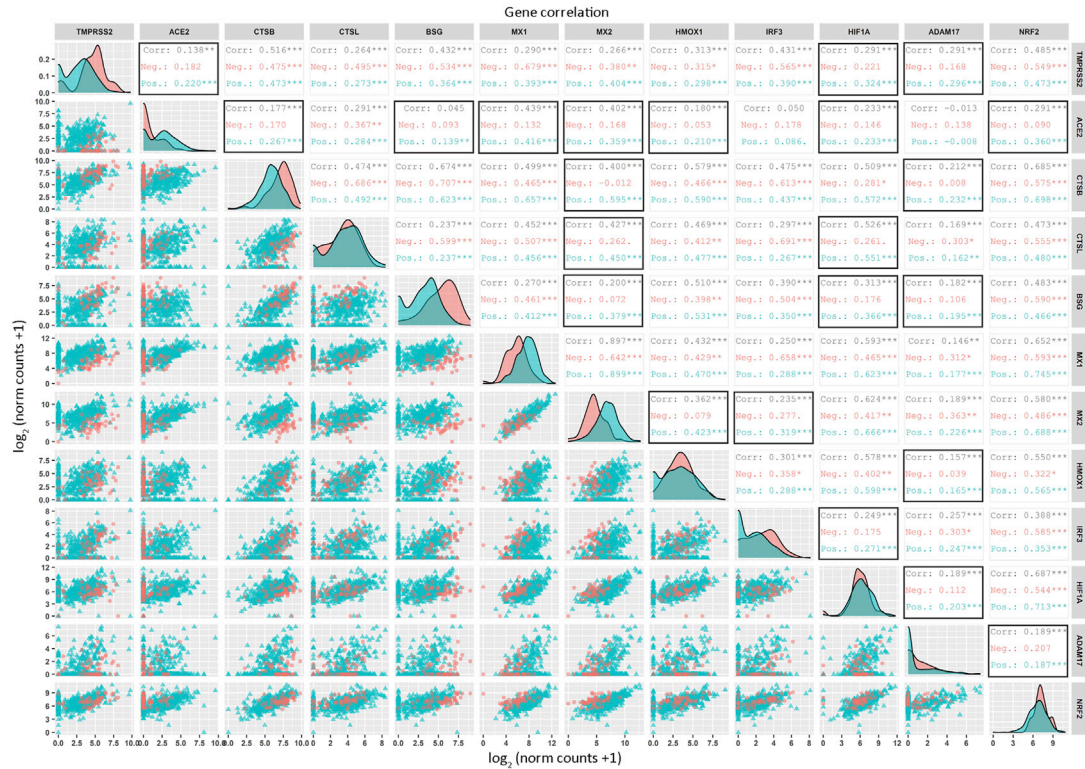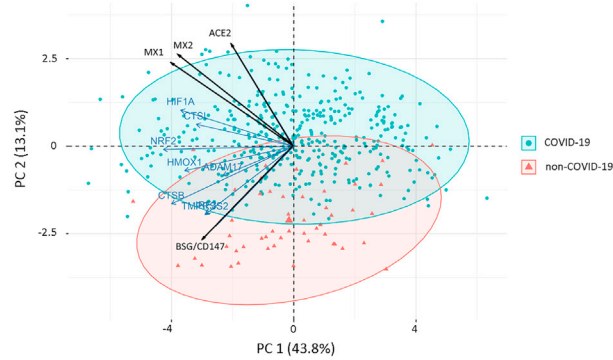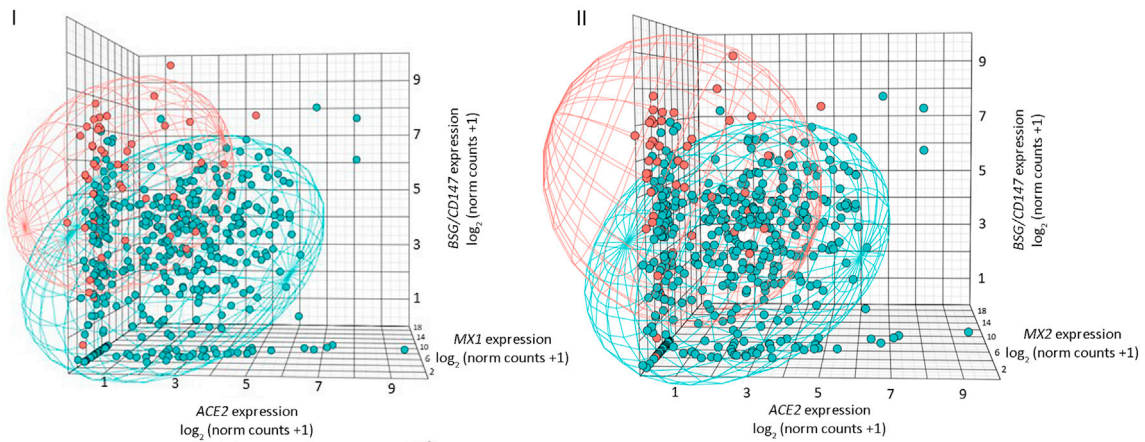
Figure 3. Gene Correlation and Principal-Component Analysis (PCA)

(A) Pairwise Spearman correlation matrix analysis between all genes of interest. The upper half displays the Spearman coefficients (r) considering all patients (Corr), non-COVID-19 patients (Neg.), or COVID-19 patients (Pos.). Black boxes highlight genes that have significant correlation only in COVID-19 patients. Statistical significance *p < 0.05; **p < 0.01; ***p < 0.001. The lower half displays the scatterplots.

(B) PCA biplot of gene expression data showing a rough segregation of non-COVID-19 and COVID-19 samples. Each point represents one individual, and the arrows depict the gene expression profile; black arrows show the 4 genes that have the greatest weight in driving the difference between the groups.

(C) 3D scatter plots for (I) *ACE2*, *MX1*, and *BSG/CD147* and (II) *ACE2*, *MX2*, and *BSG/CD147*.

Despite host cell receptors being critical targets to prevent viral infection, it is also important to consider the second line of defense in response to the pathogen. One of the antiviral effectors is MX1 (Haller et al., 2015). *MX* genes exist in nearly all vertebrate genomes, and they are active mainly against RNA viruses. MX1 is an effector protein of the IFN system (Verhelst et al., 2012; Zav'yalov et al., 2019). Studies report that MX1 generates a protective antiviral response controlling the expression of key modulator molecules associated with influenza A virus lethality; effects increased under IFN-α stimulation (Cilloniz et al., 2012; Haller et al., 2015). MX2 is also a key contributor to the type I IFN-induced post-entry inhibition of HIV-1 infection (Dicks et al., 2018). Currently, there are several ongoing clinical trials for COVID-19 prevention and/or treatment using type I or III IFNs (NCT04343976 [Phase II], NCT04385095 [Phase II], NCT04354259 [Phase II], NCT04293887 [Early Phase I], NCT04344600 [Phase II], NCT04320238 [Phase III], NCT04388709 [Phase II]). However, IFN administration could enhance a ''cyto-kine-storm'' causing a hyper-inflammatory response and contributing to multiple organ failure. Of note, recent reports showed that COVID-19 patients present a defective type I IFN response characterized by decreased production and activity, with consequent deregulation of ISGs. The authors suggest type I IFN deficiency in the blood as a hallmark of severe COVID-19 and also discuss the risk of using drugs that interfere with the IFN pathway (Hadjadj et al., 2020).

As shown in this work, *MX1* and *MX2* expression levels are higher in COVID-19 patients. Interestingly, both *MX1* and *MX2* expression increases significantly with viral load and on the contrary, their expression is reduced with age. Epidemiologic reports by the *Centers for Disease Control and Prevention (CDC)* have shown increased severity in older patients (Centers for Disease Control and Prevention, 2020). Although an important limitation of this study is the lack of clinical data accounting for disease severity, there is no correlation between age and viral load in the COVID-19 patients assessed (r = 0.031, p = 0.58). Thus, we might speculate that the loss of MX1 and MX2 with age may be associated with higher risk for severe illness.

Other ways of increasing and sustaining *MX1* expression to fight SARS-CoV-2 infection may be the use of a previously US Food and Drug Administration-approved drug known as hemin, a well-known inducer of *HMOX1*, and a modulator of *MX1* expression independent from IFN activation. Although our results show no significant alteration in *HMOX1* expression, there is sound literature referring to its interference with viral infections (Espinoza et al., 2017). Some examples include the use of CoPP, which induces *HMOX1*, promoting IRF3 phosphorylation and nuclear translocation, and subsequently expression of *MX1* (Ma et al., 2019). The protective role of *HMOX1* against viral infection has also been demonstrated for dengue, hepatitis C, hepatitis B, Ebola, Zika, and HIV-1 infections, revealing that *HMOX1* signaling pathway was a promising strategy for treating these infections (Devadas and Dhawan, 2006; Hill-Batorski et al., 2013; Huang et al., 2017; Lee et al., 2014; Protzer et al., 2007; Tseng et al., 2016). Furthermore, androg-rapholide, an anti-inflammatory and anti-oxidative compound that induces *HMOX1*, was suggested as a potential inhibitor of the main protease of SARS-CoV-2 (Enmozhi et al., 2020).

To increase the interpretability of the data we performed pairwise Spearman correlation and PCA. Results obtained were able to cluster non-COVID-19 and COVID-19 individuals based on *ACE2*, *MX1*, and *BSG/CD147* expression. Furthermore, when performing a multivariable regression analysis including viral load, age, and selected genes, *MX1* and *BSG/CD147* appear to significantly correlate with viral load independently from the other gene expressions included in the model and age. However, the increase in *MX1* compared with *BSG/CD147*, per unit of viral infection, is strikingly higher (>15-fold).

In conclusion, these results highlight *MX1* as a solid responder to SARS-CoV-2 pointing out to the relevance of evaluating approved drugs able to boost MX1 expression and halt infection. Further experimental research will be needed to ascertain the antiviral function of MX1 against SARS-CoV-2.
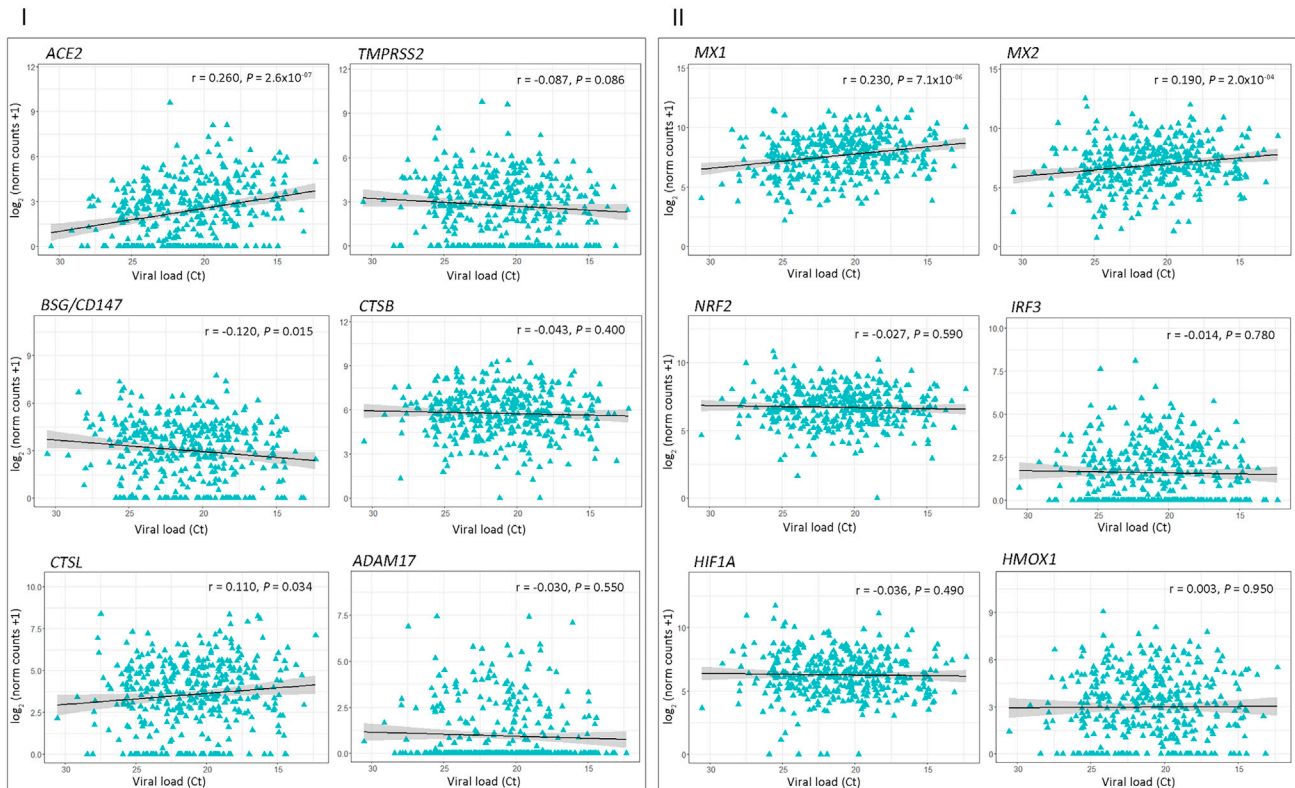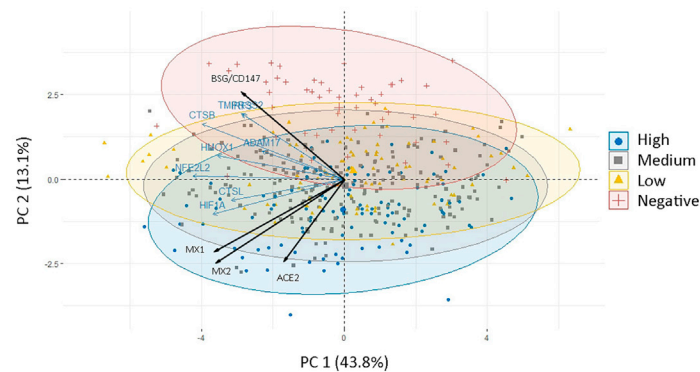
Figure 4. Correlation Analysis between Gene Expression and SARS-CoV-2 Viral Load in COVID-19 Patients

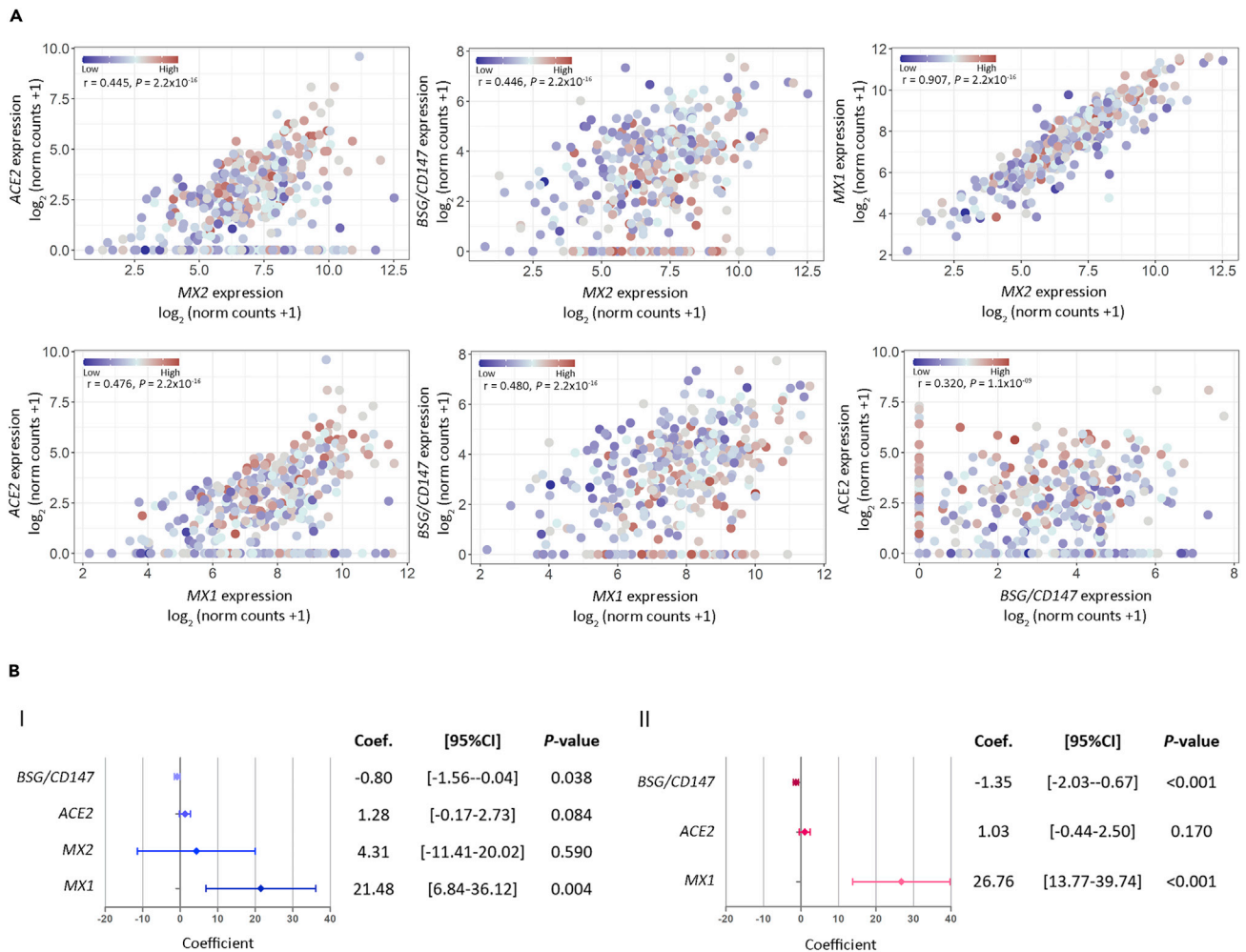(A) Viral load and gene expression correlation for (I) *ACE2, TMPRSS2, BSG/CD147, CTSB, CTSL,* and *ADAM17* and for (II) *MX1, MX2, NRF2, IRF3, HIF1A,* and *HMOX1*. Viral load was defined by the cycle threshold (Ct) of the N1 viral gene amplification during diagnostic PCR. Spearman coefficient (r) is shown for each correlation. Statistical significance was set at p < 0.05. NS: not significant.

(B) Principal-component analysis biplot of gene expression data showing a rough segregation of non-COVID-19 and COVID-19 patients stratified by low (Ct > 24), medium (Ct = 24–19), and high (Ct < 19; blue) viral load. Each point represents one individual, and the arrows depict the gene expression profile; black arrows show the 4 genes that have the greatest weight in driving the difference between the groups.

Limitations of the Study

Our analysis in this article has limitations worth mentioning. Although we performed an extensive analysis with a public RNA-seq dataset containing 484 human samples, we were not able to access complete clinical records because they are not publicly available (e.g., illness severity). In addition, RNA-seq raw data were unavailable; therefore, we were not able to perform the pre-processing and

Figure 5. Association between Viral Load and Gene Expression

(A) Dot plots representing pairwise correlations for *BSG/CD147*, *ACE2*, *MX1*, and *MX2* considering viral load in COVID-19 patients. For each comparison, the independent variable is plotted in the x axis and the dependent variable is plotted in the y axis. For all cases, viral load was considered as an independent variable. Viral load is represented as a color scale.

(B) Forest plots representing multivariable regression analysis. Model (I) considering as covariates: individual gene expression, viral load, and age; and model (II) considering as covariates: viral load, age, and all genes. Statistical significance was set at p < 0.05. NS: not significant.

alignment of sequences. However, we were able to curate samples excluding those that did not have reads for >70% of genes. Finally, some individuals suffered from other bacterial or viral infections that might confound the findings.

Resource Availability

Lead Contact

Further information and requests for resources and reagents should be directed to and will be fulfilled by the Lead Contact, Geraldine Gueron (ggueron@iquibicen.fcen.uba.ar).

Materials Availability

This study did not generate new unique reagents.

Data and Code Availability

This study did not generate new datasets.

METHODS

All methods can be found in the accompanying Transparent Methods supplemental file.

SUPPLEMENTAL INFORMATION

Supplemental Information can be found online at https://doi.org/10.1016/j.isci.2020.101585.

AUTHOR CONTRIBUTIONS

Conceptualization, J.C., E.V., and G.G.; Formal Analysis (Figures 1 and 2: J.B., S.L.-V., and S.O.; Figure 3: J.B., S.L.-V., R.L., M.A., and S.O.; Figure 4: J.B., S.L.-V., S.O., and R.L.; Figure 5: J.B., P.S., S.L.-V., and R.L.); Investigation, J.B., P.S., S.L.-V., R.L., A.S., A.T., M.A., F.C., S.O., E.V., J.C., and G.G; Resources, E.V., J.C., and G.G.; Data Curation, J.B., P.S., S.L.-V., R.L., A.S., A.T., M.A., F.C., S.O., J.C., E.V., and G.G.; Writing – Original Draft preparation, J.C., G.G., and E.V.; Writing – Review and Editing, J.B., P.S., S.L.-V., R.L., A.S., A.T., M.A., F.C., S.O., E.V., J.C., and G.G.; Funding, E.V., J.C., and G.G.; All authors have read and agreed to the published version of the manuscript.

DECLARATION OF INTERESTS

The authors declare no competing interests.

REFERENCES

Bai, Y., Yao, L., Wei, T., Tian, F., Jin, D.-Y., Chen, L., and Wang, M. (2020). Presumed asymptomatic carrier transmission of COVID-19. JAMA 323, 1406–1407.

Belouzard, S., Chu, V.C., and Whittaker, G.R. (2009). Activation of the SARS coronavirus spike protein via sequential proteolytic cleavage at two distinct sites. Proc. Natl. Acad. Sci. U S A 106, 5871–5876.

Bhargava, A., Lahaye, X., and Manel, N. (2018). Let me in: control of HIV nuclear entry at the nuclear envelope. Cytokine Growth Factor Rev. 40, 59–67.

Centers for Disease Control and Prevention. (2020). https://www.cdc.gov/coronavirus/2019-ncov/need-extra-precautions/older-adults.html.

Chiang, H.-S., and Liu, H.M. (2018). The molecular basis of viral inhibition of IRF- and STAT-dependent immune responses. Front. Immunol. 9, 3086.

Cilloniz, C., Pantin-Jackwood, M.J., Ni, C., Carter, V.S., Korth, M.J., Swayne, D.E., Tumpey, T.M., and Katze, M.G. (2012). Molecular signatures associated with Mx1-mediated resistance to highly pathogenic influenza virus infection: mechanisms of survival. J. Virol. 86, 2437–2446.

Darwish, I., Mubareka, S., and Liles, W.C. (2011). Immunomodulatory therapy for severe influenza. Expert Rev. Anti. Infect. Ther. 9, 807–822.

Devadas, K., and Dhawan, S. (2006). Hemin activation ameliorates HIV-1 infection via heme oxygenase-1 induction. J. Immunol. 176, 4252–4257.

Dicks, M.D.J., Betancor, G., Jimenez-Guardeño, J.M., Pessel-Vivares, L., Apolonia, L., Goujon, C., and Malim, M.H. (2018). Multiple components of the nuclear pore complex interact with the amino-terminus of MX2 to facilitate HIV-1 restriction. PLoS Pathog. 14, e1007408.

Enmozhi, S.K., Raja, K., Sebastine, I., and Joseph, J. (2020). Andrographolide as a potential inhibitor of SARS-CoV-2 main protease: an in silico approach. J. Biomol. Struct. Dyn. 1–7, https://doi.org/10.1080/07391102.2020.1760136.

Espinoza, J.A., González, P.A., and Kalergis, A.M. (2017). Modulation of antiviral immunity by heme oxygenase-1. Am. J. Pathol. 187, 487–493.

Glowacka, I., Bertram, S., Müller, M.A., Allen, P., Soilleux, E., Pfefferle, S., Steffen, I., Tsegaye, T.S., He, Y., Gnirss, K., et al. (2011). Evidence that TMPRSS2 activates the severe acute respiratory syndrome coronavirus spike protein for membrane fusion and reduces viral control by the humoral immune response. J. Virol. 85, 4122–4134.

Hadjadj, J., Yatim, N., Barnabei, L., Corneau, A., Boussier, J., Smith, N., Péré, H., Charbit, B., Bondet, V., Chenevier-Gobeaux, C., et al. (2020). Impaired type I interferon activity and inflammatory responses in severe COVID-19 patients. Science 369, 718–724.

Haller, O., Staeheli, P., Schwemmle, M., and Kochs, G. (2015). Mx GTPases: dynamin-like antiviral machines of innate immunity. Trends Microbiol. 23, 154–163.

Hassan, S.M., Jawad, M.J., Ahjel, S.W., Singh, R.B., Singh, J., Awad, S.M., and Hadi, N.R. (2020). The Nrf2 activator (DMF) and covid-19: is there a possible role? Med. Arch. 74, 134–138.

Heurich, A., Hofmann-Winkler, H., Gierer, S., Liepold, T., Jahn, O., and Pöhlmann, S. (2014). TMPRSS2 and ADAM17 cleave ACE2 differentially and only proteolysis by TMPRSS2 augments entry driven by the severe acute respiratory syndrome coronavirus spike protein. J. Virol. 88, 1293–1307.

Hill-Batorski, L., Halfmann, P., Neumann, G., and Kawaoka, Y. (2013). The cytoprotective enzyme heme oxygenase-1 suppresses Ebola virus replication. J. Virol. 87, 13795–13802.

Hoffmann, M., Kleine-Weber, H., Schroeder, S., Krüger, N., Herrler, T., Erichsen, S., Schiergens, T.S., Herrler, G., Wu, N.-H., Nitsche, A., et al. (2020). SARS-CoV-2 cell entry depends on ACE2 and TMPRSS2 and is blocked by a clinically proven protease inhibitor. Cell 181, 271–280.e8.

Hong, S.W., Yoo, J.W., Kang, H.S., Kim, S., and Lee, D.-K. (2009). HIF-1alpha-dependent gene expression program during the nucleic

acid-triggered antiviral innate immune responses. Mol. Cells *27*, 243–250.

Huang, H., Falgout, B., Takeda, K., Yamada, K.M., and Dhawan, S. (2017). Nrf2-dependent induction of innate host defense via heme oxygenase-1 inhibits Zika virus replication. Virology *503*, 1–5.

Jose, R.J., and Manuel, A. (2020). COVID-19 cytokine storm: the interplay between inflammation and coagulation. Lancet Respir. Med. https://doi.org/10.1016/S2213-2600(20)30216-2.

Lambert, D.W., Yarski, M., Warner, F.J., Thornhill, P., Parkin, E.T., Smith, A.I., Hooper, N.M., and Turner, A.J. (2005). Tumor necrosis factor-alpha convertase (ADAM17) mediates regulated ectodomain shedding of the severe-acute respiratory syndrome-coronavirus (SARS-CoV) receptor, angiotensin-converting enzyme-2 (ACE2). J. Biol. Chem. *280*, 30113–30119.

Lee, J.-C., Tseng, C.-K., Young, K.-C., Sun, H.-Y., Wang, S.-W., Chen, W.-C., Lin, C.-K., and Wu, Y.-H. (2014). Andrographolide exerts anti-hepatitis C virus activity by up-regulating haeme oxygenase-1 via the p38 MAPK/Nrf2 pathway in human hepatoma cells. Br. J. Pharmacol. *171*, 237–252.

Letko, M., Marzi, A., and Munster, V. (2020). Functional assessment of cell entry and receptor usage for SARS-CoV-2 and other lineage B betacoronaviruses. Nat. Microbiol. *5*, 562–569.

Li, S.-F., Gong, M.-J., Zhao, F.-R., Shao, J.-J., Xie, Y.-L., Zhang, Y.-G., and Chang, H.-Y. (2018). Type I interferons: distinct biological activities and current applications for viral infection. Cell. Physiol. Biochem. *51*, 2377–2396.

Ma, L.-L., Zhang, P., Wang, H.-Q., Li, Y.-F., Hu, J., Jiang, J.-D., and Li, Y.-H. (2019). Heme oxygenase-1 agonist CoPP suppresses influenza virus replication through IRF3-mediated generation of IFN-α/β. Virology *528*, 80–88.

Matsuyama, S., Nagata, N., Shirato, K., Kawase, M., Takeda, M., and Taguchi, F. (2010). Efficient activation of the severe acute respiratory syndrome coronavirus spike protein by the transmembrane protease TMPRSS2. J. Virol. *84*, 12658–12664.

McKimm-Breschkin, J.L. (2005). Management of influenza virus infections with neuraminidase inhibitors: detection, incidence, and implications of drug resistance. Treat. Respir. Med. *4*, 107–116.

Millet, J.K., and Whittaker, G.R. (2014). Host cell entry of Middle East respiratory syndrome coronavirus after two-step, furin-mediated activation of the spike protein. Proc. Natl. Acad. Sci. U S A *111*, 15214–15219.

Monto, A.S. (2003). The role of antivirals in the control of influenza. Vaccine *21*, 1796–1800.

Ou, X., Liu, Y., Lei, X., Li, P., Mi, D., Ren, L., Guo, L., Guo, R., Chen, T., Hu, J., et al. (2020). Characterization of spike glycoprotein of SARS-CoV-2 on virus entry and its immune cross-reactivity with SARS-CoV. Nat. Commun. *11*, 1620.

Palau, V., Riera, M., and Soler, M.J. (2020). ADAM17 inhibition may exert a protective effect on COVID-19. Nephrol. Dial. Transpl. *35*, 1071–1072.

Park, J.-E., Li, K., Barlan, A., Fehr, A.R., Perlman, S., McCray, P.B.J., and Gallagher, T. (2016). Proteolytic processing of Middle East respiratory syndrome coronavirus spikes expands virus tropism. Proc. Natl. Acad. Sci. U S A *113*, 12262–12267.

Protzer, U., Seyfried, S., Quasdorff, M., Sass, G., Svorcova, M., Webb, D., Bohne, F., Hösel, M., Schirmacher, P., and Tiegs, G. (2007). Antiviral activity and hepatoprotection by heme oxygenase-1 in hepatitis B virus infection. Gastroenterology *133*, 1156–1165.

Ramos, I., and Fernandez-Sesma, A. (2015). Modulating the innate immune response to influenza A virus: potential therapeutic use of anti-inflammatory drugs. Front. Immunol. *6*, 361.

Shulla, A., Heald-Sargent, T., Subramanya, G., Zhao, J., Perlman, S., and Gallagher, T. (2011). A transmembrane serine protease is linked to the severe acute respiratory syndrome coronavirus receptor and activates virus entry. J. Virol. *85*, 873–882.

Simmons, G., Gosalia, D.N., Rennekamp, A.J., Reeves, J.D., Diamond, S.L., and Bates, P. (2005). Inhibitors of cathepsin L prevent severe acute respiratory syndrome coronavirus entry. Proc. Natl. Acad. Sci. U S A *102*, 11876–11881.

Teijaro, J.R. (2016). Type I interferons in viral control and immune regulation. Curr. Opin. Virol. *16*, 31–40.

Tseng, C.-K., Lin, C.-K., Wu, Y.-H., Chen, Y.-H., Chen, W.-C., Young, K.-C., and Lee, J.-C. (2016). Human heme oxygenase 1 is a potential host cell factor against dengue virus replication. Sci. Rep. *6*, 32176.

Ulrich, H., and Pillat, M.M. (2020). CD147 as a target for COVID-19 treatment: suggested effects of azithromycin and stem cell engagement. Stem Cell Rev. Rep. 1–7, https://doi.org/10.1007/s12015-020-09976-7.

Vaduganathan, M., Vardeny, O., Michel, T., McMurray, J.J.V., Pfeffer, M.A., and Solomon, S.D. (2020). Renin-angiotensin-aldosterone system inhibitors in patients with covid-19. N. Engl. J. Med. *382*, 1653–1659.

van Doremalen, N., Bushmaker, T., Morris, D.H., Holbrook, M.G., Gamble, A., Williamson, B.N., Tamin, A., Harcourt, J.L., Thornburg, N.J., Gerber, S.I., et al. (2020). Aerosol and surface stability of SARS-CoV-2 as compared with SARS-CoV-1. N. Engl. J. Med. https://doi.org/10.1056/NEJMc2004973.

Verhelst, J., Parthoens, E., Schepens, B., Fiers, W., and Saelens, X. (2012). Interferon-inducible protein Mx1 inhibits influenza virus by interfering with functional viral ribonucleoprotein complex assembly. J. Virol. *86*, 13445–13455.

Wang, K., Chen, W., Zhou, Y.-S., Lian, J.-Q., Zhang, Z., Du, P., Gong, L., Zhang, Y., Cui, H.-Y., Geng, J.-J., et al. (2020). SARS-CoV-2 invades host cells via a novel route: CD147-spike protein. bioRxiv. https://doi.org/10.1101/2020.03.14.988345.

World Health Organization. (2020). Novel coronavirus (2019-nCoV) situation report - 1. https://www.who.int/docs/default-source/coronaviruse/situation-reports/20200121-sitrep-1-2019-ncov.pdf?sfvrsn=20a99c10_4.

Yan, R., Zhang, Y., Li, Y., Xia, L., Guo, Y., and Zhou, Q. (2020). Structural basis for the recognition of SARS-CoV-2 by full-length human ACE2. Science *367*, 1444–1448.

Zav'yalov, V.P., Hämäläinen-Laanaya, H., Korpela, T.K., and Wahlroos, T. (2019). Interferon-Inducible myxovirus resistance proteins: potential biomarkers for differentiating viral from bacterial infections. Clin. Chem. *65*, 739–750.

Zheng, B.-J., Chan, K.-W., Lin, Y.-P., Zhao, G.-Y., Chan, C., Zhang, H.-J., Chen, H.-L., Wong, S.S.Y., Lau, S.K.P., Woo, P.C.Y., et al. (2008). Delayed antiviral plus immunomodulator treatment still reduces mortality in mice infected by high inoculum of influenza A/H5N1 virus. Proc. Natl. Acad. Sci. U S A *105*, 8091–8096.

Zheng, Z., Peng, F., Xu, B., Zhao, J., Liu, H., Peng, J., Li, Q., Jiang, C., Zhou, Y., Liu, S., et al. (2020). Risk factors of critical & mortal COVID-19 cases: a systematic literature review and meta-analysis. J. Infect. *81*, e16–e25.

Zhou, Y., Vedantham, P., Lu, K., Agudelo, J., Carrion, R.J., Nunneley, J.W., Barnard, D., Pöhlmann, S., McKerrow, J.H., Renslo, A.R., and Simmons, G. (2015). Protease inhibitors targeting coronavirus and filovirus entry. Antivir. Res. *116*, 76–84.

Zou, L., Ruan, F., Huang, M., Liang, L., Huang, H., Hong, Z., Yu, J., Kang, M., Song, Y., Xia, J., et al. (2020). SARS-CoV-2 viral load in upper respiratory specimens of infected patients. N. Engl. J. Med. https://doi.org/10.1056/NEJMc2001737.

Supplemental Information

SARS-CoV-2 Infection Boosts *MX1* Antiviral

Effector in COVID-19 Patients

Juan Bizzotto, Pablo Sanchis, Mercedes Abbate, Sofía Lage-Vickers, Rosario Lavignolle, Ayelén Toro, Santiago Olszevicki, Agustina Sabater, Florencia Cascardo, Elba Vazquez, Javier Cotignola, and Geraldine Gueron

Table S1. Patient demographics for the GSE152075 dataset. Related to all figures.

		non-COVID-19	COVID-19	*P*-value
Number of patients		50	403	
Sex	**Male**	22 (44%)	166 (41.2%)	
	Female	28 (56%)	187 (46.4%)	0.763 [a]
	Unknown	-	50 (12.4%)	
Age (years)	**Range**	12 - 91	2 - 91	
	Inter Quartile Range	29-63	41-71	
	Median	46.5	56	
	Media	46.5	55.6	0.002 [b]
	<30s	13 (26%)	41 (10.2%)	
	30s	5 (10%)	51 (12.7%)	
	40s	10 (20%)	55 (13.6%)	
	50s	7 (14%)	80 (19.9%)	
	60s	8 (16%)	50 (12.4%)	
	$\geq$70	7 (14%)	110 (27.3%)	0.012 [c]
	Unknown	-	16 (3.9%)	
Viral load	**High (Ct <19)**	-	106 (26.3%)	
	Mid (Ct 19-24)	-	197 (48.9%)	
	Low (Ct >24)	-	84 (20.9%)	
	Unknown	-	16 (3.9%)	

Table contains the number and % of COVID-19 and non-COVID-19 patients according to sex, age and viral load. [a] Fisher's exact; [b] t-Student test; [c] Chi-square test.

Table S2. Host receptor and antiviral gene correlation in all patients (Global), non-COVID-19 patients, or COVID-19 patients. Related to Figure 3A.

Genes		Global		Negative (non-COVID-19)		Positive (COVID-19)	
		r	*P*-value	r	*P*-value	r	*P*-value
ACE2	ADAM17	-0.013	0.786	0.138	0.340	-0.008	0.878
	BSG	0.045	0.343	0.093	0.522	**0.139**	**0.005**
	CTSB	0.177	1.59×10^{-04}	0.170	0.237	**0.267**	**5.22×10^{-08}**
	CTSL	0.291	2.85×10^{-10}	0.367	0.009	0.284	6.19×10^{-09}
	HIF1A	0.233	5.61×10^{-07}	0.146	0.312	**0.233**	**2.28×10^{-06}**
	HMOX1	0.180	1.15×10^{-04}	0.053	0.714	**0.210**	**2.22×10^{-05}**
	IRF3	0.050	0.284	0.178	0.217	0.086	0.084
	MX1	0.439	$<1 \times 10^{-15}$	0.132	0.361	**0.416**	**$<1 \times 10^{-15}$**
	MX2	0.402	$<1 \times 10^{-15}$	0.168	0.244	**0.359**	**1.07×10^{-13}**
	NRF2	0.291	2.82×10^{-10}	0.090	0.534	**0.360**	**8.22×10^{-14}**
ADAM17	NRF2	0.189	5.17×10^{-05}	0.207	0.150	**0.187**	**1.57×10^{-04}**
BSG	ADAM17	0.182	9.70×10^{-05}	0.106	0.464	**0.195**	**8.27×10^{-05}**
	HIF1A	0.313	1.01×10^{-11}	0.176	0.221	**0.366**	**3.26×10^{-14}**
	HMOX1	0.510	$<1 \times 10^{-15}$	0.398	0.004	0.531	$<1 \times 10^{-15}$
	IRF3	0.390	$<1 \times 10^{-15}$	0.504	1.92×10^{-04}	0.350	5.01×10^{-13}
	MX1	0.270	5.52×10^{-09}	0.461	0.001	0.412	$<1 \times 10^{-15}$
	MX2	0.200	1.76×10^{-05}	0.072	0.617	**0.379**	**3.55×10^{-15}**
	NRF2	0.483	$<1 \times 10^{-15}$	0.590	6.59×10^{-06}	0.466	$<1 \times 10^{-15}$
CTSB	ADAM17	0.212	5.07×10^{-06}	0.008	0.954	**0.232**	**2.55×10^{-06}**
	BSG	0.674	$<1 \times 10^{-15}$	0.707	9.88×10^{-09}	0.623	$<1 \times 10^{-15}$
	CTSL	0.474	$<1 \times 10^{-15}$	0.686	3.91×10^{-08}	0.492	$<1 \times 10^{-15}$
	HIF1A	0.509	$<1 \times 10^{-15}$	0.281	0.048	0.572	$<1 \times 10^{-15}$
	HMOX1	0.579	$<1 \times 10^{-15}$	0.466	0.001	0.590	$<1 \times 10^{-15}$
	IRF3	0.475	$<1 \times 10^{-15}$	0.613	2.26×10^{-06}	0.437	$<1 \times 10^{-15}$
	MX1	0.499	$<1 \times 10^{-15}$	0.465	0.001	0.657	$<1 \times 10^{-15}$
	MX2	0.400	$<1 \times 10^{-15}$	-0.012	0.933	**0.595**	**$<1 \times 10^{-15}$**
	NRF2	0.685	$<1 \times 10^{-15}$	0.575	1.24×10^{-05}	0.698	$<1 \times 10^{-15}$

Genes		Global		Negative (non-COVID-19)		Positive (COVID-19)	
		r	*P*-value	r	*P*-value	r	*P*-value
CTSL	ADAM17	0.169	2.91×10^{-04}	0.303	0.033	0.162	0.001
	BSG	0.237	3.31×10^{-07}	0.599	4.41×10^{-06}	0.237	1.56×10^{-06}
	HIF1A	0.526	$<1 \times 10^{-15}$	0.261	0.067	**0.551**	**$<1 \times 10^{-15}$**
	HMOX1	0.469	$<1 \times 10^{-15}$	0.412	0.003	0.477	$<1 \times 10^{-15}$
	IRF3	0.297	1.14×10^{-10}	0.691	2.85×10^{-08}	0.267	5.37×10^{-08}
	MX1	0.452	$<1 \times 10^{-15}$	0.507	1.71×10^{-04}	0.456	$<1 \times 10^{-15}$
	MX2	0.427	$<1 \times 10^{-15}$	0.262	0.066	**0.450**	**$<1 \times 10^{-15}$**
	NRF2	0.473	$<1 \times 10^{-15}$	0.555	2.94×10^{-05}	0.480	$<1 \times 10^{-15}$
HIF1A	ADAM17	0.189	5.40×10^{-05}	0.112	0.438	**0.203**	**4.09×10^{-05}**
	NRF2	0.687	$<1 \times 10^{-15}$	0.544	4.39×10^{-05}	0.713	$<1 \times 10^{-15}$
HMOX1	ADAM17	0.157	0.001	0.039	0.786	**0.165**	**0.001**
	HIF1A	0.578	$<1 \times 10^{-15}$	0.402	0.004	0.598	$<1 \times 10^{-15}$
	IRF3	0.301	5.88×10^{-11}	0.358	0.011	0.288	4.03×10^{-09}
	NRF2	0.550	$<1 \times 10^{-15}$	0.322	0.023	0.565	$<1 \times 10^{-15}$
IRF3	ADAM17	0.257	2.99×10^{-08}	0.303	0.032	0.247	5.21×10^{-07}
	HIF1A	0.249	7.95×10^{-08}	0.175	0.223	**0.271**	**3.11×10^{-08}**
	NRF2	0.388	$<1 \times 10^{-15}$	0.585	8.01×10^{-06}	0.353	2.8×10^{-13}
MX1	ADAM17	0.146	0.002	0.312	0.028	0.177	3.64×10^{-04}
	HIF1A	0.593	$<1 \times 10^{-15}$	0.465	0.001	0.623	$<1 \times 10^{-15}$
	HMOX1	0.432	$<1 \times 10^{-15}$	0.429	0.002	0.470	$<1 \times 10^{-15}$
	IRF3	0.250	7.28×10^{-08}	0.658	2.08×10^{-07}	0.288	3.90×10^{-09}
	MX2	0.897	$<1 \times 10^{-15}$	0.642	4.97×10^{-07}	0.899	$<1 \times 10^{-15}$
	NRF2	0.652	$<1 \times 10^{-15}$	0.593	5.66×10^{-06}	0.745	$<1 \times 10^{-15}$
MX2	ADAM17	0.189	4.94×10^{-05}	0.363	0.01	0.226	4.48×10^{-06}
	HIF1A	0.624	$<1 \times 10^{-15}$	0.417	0.003	0.666	$<1 \times 10^{-15}$
	HMOX1	0.362	1.78×10^{-15}	0.079	0.587	**0.423**	**$<1 \times 10^{-15}$**
	IRF3	0.235	4.42×10^{-07}	0.277	0.051	**0.319**	**5.61×10^{-11}**
	NRF2	0.580	$<1 \times 10^{-15}$	0.486	$<1 \times 10^{-15}$	0.688	$<1 \times 10^{-15}$

Genes		Global		Negative (non-COVID-19)		Positive (COVID-19)	
		r	*P*-value	r	*P*-value	r	*P*-value
TMPRSS2	ACE2	0.138	0.003	0.182	0.206	**0.220**	**8.66×10^{-06}**
	ADAM17	0.291	2.68×10^{-10}	0.168	0.243	**0.296**	**1.43×10^{-09}**
	BSG	0.432	$<1 \times 10^{-15}$	0.534	6.55×10^{-05}	0.364	4.71×10^{-14}
	CTSB	0.516	$<1 \times 10^{-15}$	0.475	4.87×10^{-04}	0.473	$<1 \times 10^{-15}$
	CTSL	0.264	1.22×10^{-08}	0.495	2.61×10^{-04}	0.273	2.67×10^{-08}
	HIF1A	0.291	2.64×10^{-10}	0.221	0.123	**0.324**	**2.51×10^{-11}**
	HMOX1	0.313	8.95×10^{-12}	0.315	0.026	0.298	1.03×10^{-09}
	IRF3	0.431	$<1 \times 10^{-15}$	0.565	1.95×10^{-05}	0.390	4.44×10^{-16}
	MX1	0.290	3.35×10^{-10}	0.679	5.88×10^{-08}	0.393	2.22×10^{-16}
	MX2	0.266	9.16×10^{-09}	0.380	0.006	0.404	$<1 \times 10^{-15}$
	NRF2	0.485	$<1 \times 10^{-15}$	0.549	3.63×10^{-05}	0.473	$<1 \times 10^{-15}$

Table contains the r value and *P*-value for gene correlations. Genes that have significant correlation in COVID-19 patients but non-significant correlation in non-COVID-19 are highlighted in bold. Data was taken from the GSE152075 dataset.

TRANSPARENT METHODS

Transcriptome datasets selection and study population

We browsed the Gene Expression Omnibus (GEO) repository (Barrett et al., 2013) using the following keywords and expressions: [(COVID) OR (COVID-19) OR (CORONAVIRUS) OR (SARS-CoV-2) OR (2019-nCoV)] AND [(transcriptomics) OR (RNA-seq) OR (microarray) OR (expression) OR (transcriptome)]. All potentially relevant datasets were further evaluated in detail by 2-3 authors. The eligibility criteria included: (i) publicly available transcriptome data; (ii) detailed sample information; (iii) detailed protocol information; (iv) ≥ 60 samples.

We selected the GSE152075 dataset, which contains RNA-seq data from 430 SARS-CoV-2 positive and 54 negative patients (Lieberman et al., 2020). RNA was isolated from nasopharyngeal swabs and sequenced in an Illumina NextSeq 500 instrument. Reads were

pseudoaligned to the human transcriptome and pre-processed by the authors of the original study (Lieberman et al., 2020). Clinico-pathological information included age, sex, and viral load (expressed as cycle threshold (Ct) by RT-qPCR for the N1 viral gene at time of diagnosis). The interpretation for viral load was: the higher the viral load, the lower de Ct.

RNA-seq analysis

We downloaded the pseudoaligned and pre-processed RNA-seq data. We removed samples with >70% of total genes with 0 sequences reads considering them as very low-quality samples that might introduce a bias. Normalization, batch effect correction and differential expression were performed with R package DEseq2 v1.28.1 (Love et al., 2014).

Statistical analyses

Wilcoxon rank sum test was performed to determine statistical differences between categorical groups. Age was categorized according to the WHO guidelines ("World Health Organization 2020 - Novel Coronavirus (2019-nCoV) Situation Report - 1," n.d.): <30 years old, every 10 years between 30-70 years old and ≥70 years old. Two-sided, increasing and decreasing Jonckheere-Terpstra trend tests (with 500 permutations) were used to determine statistical trends between gene expression and age groups. To study pairwise correlations between continuous variables, Spearman's rank correlation coefficient was calculated. Multilinear regression analyses were performed to determine the correlation between the expression of two genes and viral load. To estimate the regression coefficients of the different models, we used a multivariable regression including gene expression, viral load and age as covariates.

All statistical analyses were done in Stata v14 (StataCorp LLC, College Station, TX, USA) or GraphPad Prism (La Jolla, CA, USA). Statistical significance was set as $P < 0.05$. We did not correct P value for multiple testing.

Principal Component Analysis (PCA) was done with the factorextra and dplyr packages in R (Kassambara and Mundt, 2020). We included only the selected host receptors and antiviral genes.

All results were plotted using ggplot2 (Wickham and Hadley, 2016), ggpubr (Kassambara, 2020), GGally (Schloerke et al., 2020), canvasXpress (Neuhaus and Brett, 2020) in R, or GraphPad Prism (La Jolla, CA, USA).

SUPLEMENTARY REFERENCES

Barrett, T., Wilhite, S.E., Ledoux, P., Evangelista, C., Kim, I.F., Tomashevsky, M., Marshall, K.A., Phillippy, K.H., Sherman, P.M., Holko, M., Yefanov, A., Lee, H., Zhang, N., Robertson, C.L., Serova, N., Davis, S., Soboleva, A., 2013. NCBI GEO: archive for functional genomics data sets--update. Nucleic Acids Res. 41, D991-5. https://doi.org/10.1093/nar/gks1193

Kassambara, A., 2020. ggpubr: "ggplot2" Based Publication Ready Plots.

Kassambara, A., Mundt, F., 2020. factoextra: Extract and Visualize the Results of Multivariate Data Analyses. R package.

Lieberman, N.A.P., Peddu, V., Xie, H., Shrestha, L., Huang, M.-L., Mears, M.C., Cajimat, M.N., Bente, D.A., Shi, P.-Y., Bovier, F., Roychoudhury, P., Jerome, K.R., Moscona, A., Porotto, M., Greninger, A.L., 2020. In vivo antiviral host response to SARS-CoV-2 by viral load, sex, and age. bioRxiv Prepr. Serv. Biol. 2020.06.22.165225. https://doi.org/10.1101/2020.06.22.165225

Love, M.I., Huber, W., Anders, S., 2014. Moderated estimation of fold change and dispersion for RNA-seq data with DESeq2. Genome Biol. 15, 550. https://doi.org/10.1186/s13059-014-0550-8

Neuhaus, I., Brett, C., 2020. canvasXpress: Visualization Package for CanvasXpress in R.

Schloerke, B., Cook, D., Larmarange, J., Francois, B., Marbach, M., Thoen, E., Elberg, A.,

    Crowley, J., 2020. GGally: Extension to "ggplot2". R package.

Wickham, Hadley, 2016. ggplot2. Elegant Graphics for Data Analysis. Springer-Verlag, NY.

World Health Organization 2020 - Novel Coronavirus (2019-nCoV) Situation Report - 1

    [WWW Document], n.d. URL https://www.who.int/docs/default-

    source/coronaviruse/situation-reports/20200121-sitrep-1-2019-

    ncov.pdf?sfvrsn=20a99c10_4